Size Dependence of the Kinetic Rate Constant for Phase Transformation in TiO2 Nanoparticles

ARTICLE *in* CHEMISTRY OF MATERIALS · MAY 2005

Impact Factor: 8.35 · DOI: 10.1021/cm0508423

2 AUTHORS, INCLUDING:

Hengzhong Zhang
University of California, Berkeley
77 PUBLICATIONS **5,653** CITATIONS

SEE PROFILE

Chem. Mater. 2005, 17, 3421

Size-dependence of the kinetic rate constant for phase transformation in TiO_2 nanoparticles

Hengzhong Zhang, Jillian F. Banfield

TOC Graphic

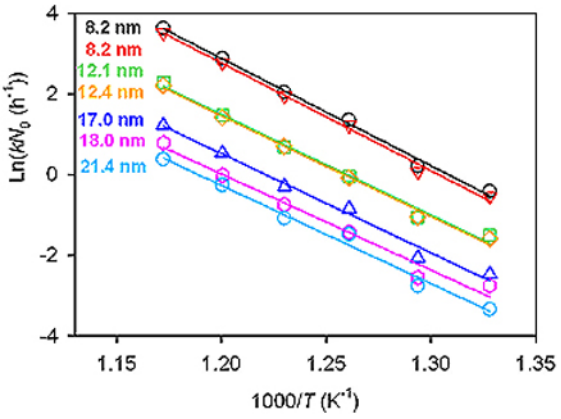

Arrhenius plot revealing a strong size dependence of the rate constant for the phase transformation from nanocrystalline anatase to rutile.

Keywords: nanocrystalline, titania, kinetics, rate constant, particle size

Size-dependence of the kinetic rate constant for phase transformation in TiO_2 nanoparticles

Hengzhong Zhang[1 *], *Jillian F. Banfield* [1]

[1] Department of Earth and Planetary Science, University of California Berkeley, Berkeley, California 94720

* Corresponding author, E-mail: heng@eps.berkeley.edu, phone: 510-643-9120, Fax: 510-643-9980.

Abstract: The temperature dependence of a kinetic rate constant for a phase transformation is usually described by the Arrhenius equation, which comprises a pre-exponential factor multiplied by an exponential term involving activation energy and temperature. In this work we show that particle size is another factor that is needed in description of kinetics of phase transformations in nanoparticles. For phase transformation in nanocrystalline titania (TiO_2) proceeding via nucleation at particle-particle contacts, the activation energy varies slightly with particle size but the pre-

exponential factor is inversely proportional to the approximately fourth power of the particle size. We attribute the large pre-exponential factor primarily to the high concentration of nucleation sites at particle-particle interfaces in nanomaterials compared to bulk materials. We proposed a kinetic equation that incorporates dependence of the rate constant on the particle size for phase transformation via interface nucleation in nanoparticles.

Introduction

Titania (TiO_2) is a wide bandgap (~ 3.2 eV) semiconductor. Its optoelectronic and photochemical properties such as photocatalytic ability are influenced by its phase structure (e.g. anatase vs. rutile) and particle size[1, 2]. Thus study the phase transformation in TiO_2 nanoparticles is fundamental to the applications.

Descriptions of phase transformation kinetics typically include temperature, pressure, magnetic field, and chemical environment, but rarely consider explicitly the effects of particle size. However, the effects of size on reaction kinetics in some micron-scale materials have been investigated. These studies have shown that particle size can affect the apparent activation energy and the pre-exponential factor by changing the reaction mechanism[1,4]. The question of size effects on phase transformation behavior may be even more relevant for nanomaterials than for micron-sized materials. The impact of size on the kinetics of pressure-induced phase transformations in nanometer-scale particles has been examined.[5,6,7] However, the effects of small size on the kinetics of thermally-driven transformations are less well studied, largely because of the challenge of dealing simultaneously with phase transformation and coarsening. The size effects on reaction kinetics in nanomaterials may be particularly relevant because transformations can

proceed at lower temperatures than in related bulk materials, thus in a temperature regime where nano-scale size is retained. Particle size can dramatically impact the rate of phase transformations in nanoparticles if nucleation of the product occurs at particle-particle contacts and the rate is not limited by growth of the nuclei.[8] This is the case for the transformation from nanoparticulate anatase to rutile, which has been shown to depend upon particle size because size controls the number of particle-particle contacts per unit volume.[9,10] Size can be incorporated explicitly into expressions to describe the kinetics of the phase transformations. The kinetic equation used to describe the transformation of nanocrystalline anatase to rutile at short reaction times and <600 ^{o}C is [9,10]:

$$-\frac{dN}{dt} = kN^2 \qquad (1a)$$

where N is the numbers of nanoparticles of anatase in a sample at time t and k is the rate constant for the phase transformation from nanocrystalline anatase to rutile. The integrated form is:

$$\ln\left[\frac{(D/D_0)^3}{\alpha} - 1\right] = \ln(kN_0) + \ln t \qquad (1b)$$

where N_0 is N at the start of the experiment, D_0 and D are the average particle diameters of anatase at t = 0 and t, and α is the weight fraction of anatase (α = 1-w.t.(rutile)/100). N_0 in a given volume is proportional to $1/D_0^3$ for anatase samples of different initial sizes. Eq 1 can be viewed as a second order kinetic equation because the rate depends on the

probability of particle contacts. The formulation is analogous to that for a molecular reaction that requires collision between two molecules. Here we use eq 1b to explore particle size effects on the activation energy and the pre-exponential factor for the phase transformation of nanocrystalline anatase to rutile. We report a strong size dependence of the pre-exponential factor and provide an explanation for this phenomenon.

Experimental Section

Preparation of nanocrystalline anatase. Samples of nanocrystalline anatase of different average sizes (~ 8-21 nm) were prepared by heating nanometer-sized amorphous titania at various temperatures.[11] Nanometer-sized amorphous titania powders were produced by hydrolysis of titanium ethoxide in water at 0 ^{o}C. Sub-samples of the amorphous titania were heated in air for 3 h at several temperatures between 375 ^{o}C and 550 ^{o}C, producing amorphous-free single-phase nanocrystalline anatase of various average particle sizes in the range 8 – 21 nm, as determined from x-ray diffraction (XRD) data using the Scherrer equation[10,12]. Transmission electron microscopy examination showed that the nanoparticles are close to spherical. [11]

X-ray diffraction. A Scintag PADV diffractometer with Cu K_{α} radiation (λ = 1.5419 Å) operated at 35 kV and 40 mA was used to collect x-ray diffraction patterns of nanoparticles dispersed on a low background quartz plate.

Determination of specific surface area. An Accelerated Surface Area and Porosimetry System (Micrometrics ASAP 2010) was used to determine the adsorption / desorption isotherms of nitrogen gas at 77 K on nanocrystalline anatase samples. The Brunauer-Emmett-Teller (BET) equation was used to calculate the specific surface areas

of samples from the adsorption isotherms. The pore size distribution was calculated using the Barrett-Johner-Halenda (BJH) method [13].

Kinetic experiments. Samples of anatase ca. 40 mg each were put into small alumina crucibles and then heated in air at temperatures between 480 and 580 ^{o}C at an interval of 20 ^{o}C for different periods of time. The phase contents and the average particle sizes of the nanophases of the heated samples were analyzed using XRD data following the approach from the literature. [10,12]

Results and Discussion

Figures 1a and 1b show the rutile contents and the average particle sizes of anatase in samples heated at 520 ^{o}C, respectively. Experimental data at other temperatures are documented in Supporting Information (Figure S1). It is important to note that each of the initial anatase samples used in these experiments differ both in particle size and in aggregation state. As the rate depends on both of these factors, Figure 1a and Figure S1 do not show simple trends with time for samples of similar average sizes. The size dependence can only be deduced through the kinetic analyses using eq 1 to consider both variables.

The specific surface areas of two ~ 12 nm anatase samples were determined to be 86.2 ± 1.2 m^2/g (12.4 nm) and 97.0 ± 1.3 m^2/g (12.1 nm), respectively (Ref. Supporting Information, Figure S3). The difference in surface area is attributed to difference in packing density or the aggregation state of the nanoparticles. The higher surface area (lower packing density) explains the lower reactivity of one of the two samples of the

same average particle size, as indicated in Figure 1a and Figures S1a,c,e,g,i of Supporting Information (green data points vs. yellow data points).

Kinetic plots of the data (Figure 1c and Figure S2 of Supporting Information) show linear relationships between values for the left side of eq 1b and ln *t* at short reaction times (data at long reaction times are not included in the fit because coarsening rates for rutile become significant when the particle size increases[9]). At 520 ^{o}C, the kN_0 of the 21.4 nm anatase sample is close to that of the 18.0 nm sample (i.e. the exp(intercept) of the blue line is close to that of the pink line in Figure 1c). This is probably caused by experimental errors in the determination of the XRD data of the 21.4 nm anatase sample. Since the aggregation states (Table S1, Supporting Information) and the initial sizes of the two samples are different, their rate constants (kN_0) should be different, as observed at other temperatures (Figure S2).

The intercepts of the regression lines (Figure 1c and Figure S2) increase significantly as the initial size decreases, revealing a strong size-dependence of the rate constant, *k*. The derived rate constants (kN_o) are summarized in Figure 2a. The relationship between the rate constant and temperature is described by the Arrhenius equation:

$$\ln(kN_0) = \ln(f_0 N_0) - \frac{E_a}{RT} \qquad (2)$$

where f_0 is the pre-exponential factor, E_a is the activation energy, R is the gas constant (8.314 J/mol·K), and T is temperature. From an Arrhenius plot, the apparent pre-exponential factor, f_0N_0, is calculated from the exp(intercept) and the activation energy, E_a, from - slope·R. Results (Figures 2b and 2c) show that particle size causes slight

changes in the activation energy but large changes in the apparent pre-exponential factor. In the following, we consider explanations for the observed particle size effects on the activation energy and the pre-exponential factor.

At a solid surface, coordination numbers of atoms are generally lower than those in the bulk. Due to the reduced coordination, forces exerted on surface atoms from neighbors are unbalanced in the direction normal to the surface, generating a net force acting upon atoms in the interior of the solid. The magnitude of the force on the surface per unit length is termed surface stress, f .[14] In a small solid particle, the unbalanced forces existing on the surface produce an excess pressure (P_{exc}) acting upon the whole solid particle: [14, 15]

$$P_{exc} = \frac{4f}{D_0} \qquad (3)$$

In anatase nanoparticles, the excess pressure compresses the particle, resulting in a contraction in the Ti-O bond, as revealed by conventional x-ray diffraction study [16] and synchrotron x-ray absorption near edge structure (XANES) study [17], and hence a stronger binding between Ti and O atoms. The effect is likely to be most pronounced at the surface. As a consequence, more thermal energy is needed to break and rearrange bonds to nucleate rutile at nanoparticle surfaces. This causes an increase in the activation energy that can be assumed to be proportional to the excess pressure. That is,

$$E_a = E_a(\infty) + c'\frac{4f}{D_0} = E_a(\infty) + \frac{c}{D_0} \quad (4)$$

where $E_a(\infty)$ is the activation energy for interface nucleation in bulk anatase and c' and c are proportional coefficients. A similar equation was given by Talapin et al. for crystal growth of nanoparticles in a solution, based on a consideration of the system energy shifted by the particle size[18]. According to eq 4, a linear relationship exists between the activation energy and the reciprocal particle size, as illustrated in Figure 2b. Linear least square regression gave $E_a(\infty)$ = 185.1 ± 2.8 kJ/mol (standard errors determined by regression) and c = 293.3 ± 29.5 kJ · nm/mol (c is proportional to surface stress) with a regression coefficient = 0.956. The difference in E_a for particles of 5 nm vs. 100 nm in diameter is ~ 60 kJ/mol.

A log-log plot of the apparent pre-exponential factor vs. the initial particle size (Figure 2c) yields the following empirical linear relationship by regression, with a regression coefficient = 0.991:

$$\ln(f_0 N_0) = (48.4 \pm 1.4) - (6.7 \pm 0.6)\ln D_0 \quad (5)$$

where $f_0 N_0$ is in the unit of 1/h and D_0 in nm. The slope of above equation is -6.7± 0.6, indicating a strong dependence of the apparent pre-exponential factor on particle size, i.e., $f_0 N_0 \propto 1/D_0^{\,6.7\pm0.6}$. Given N_0 is $\propto 1/D_0^3$, then f_0 is inferred to be $\propto 1/D_0^{3.7\pm0.6}$. In the following we explore the physical significance of the dependence of f_0 on D_0.

The pre-exponential factor is proportional to the product of the vibrational frequency (v, the frequency with which atoms attempt the transformation) and the natural exponent of the entropy of activation.[19] For nanoparticles, v may differ from that of bulk materials. This effect is likely to be most pronounced for atoms at surfaces, changing their probability of achieving the activated state in a given time relative to bulk material. Measurements of how v varies with size are not available. However, the lattice vibrational frequency in 3 nm ZnS was estimated to be ~ 1.6 times larger than of bulk ZnS [20]. Although not directly applicable, the result suggests that the size effect on v, thus on f_0 is minimal compared to the observed dependence of f_0 on particle size.

The configurational entropies of the initial and activated states in nanoparticles may be size dependent. Because nanoparticles have a high concentration of distorted edge and corner sites, especially when particles are very small, the configurational entropy of the initial (and perhaps activated) state may be higher than that of bulk material. However, the difference probably does not vary strongly with size, and alone is unlikely to explain the observed strong inverse relationship between size and the pre-exponential factor.

As neither of the conventional contributors (vibrational frequency and configurational entropy) appears to be able to account for the observed change in the pre-exponential factor with particle size, it is necessary to consider additional factors that are relevant in nanomaterials. For interface nucleation in nanoparticles, the pre-exponential factor determined from eq 1 must also depend linearly upon the number of particle-particle contacts with surface geometries optimally configured for transformation, N_1.[21] In other words, N_1 is a measure of the concentration of interface nucleation sites. For an anatase sample of a unit volume, the smaller the initial particle size (D_0), the larger N_0, and N_1.

Assuming a linear relationship between N_1 to N_0, then $f_0 \propto 1/D_0^3$ because $f_0 \propto N_1 \propto N_0$ and $N_0 \propto 1/D_0^3$.

A dependence of the pre-exponential factor on particle size has been documented previously for a chemical reaction. The frequency factor for oxidation of 40 nm soot was determined to be about four times smaller than that of 130 nm soot (the activation energy was assumed constant).[22] This effect is very small compared to that observed in nano-sized titania. This difference is to be expected, given that the pre-exponential factor for chemical reactions depends only on v and the configurational entropy.

As the predicted dependence of f_0 on N_1 is $\propto 1/D_0^3$ while the observed dependence of f_0 on size is $\propto 1/D_0^{3.7\pm 0.6}$, we infer that the change in configurational entropy, and possibly v, with size may modify f_0 by $\sim 1/D^{0.7\pm 0.6}$. This supports above assessment that the difference in the configurational entropy is probably not a strong function of particle size.

Taking into account the size dependences of the activation energy (eq 4) and the pre-exponential factor (eq 5), the kinetic equation eq 1a for phase transformation in nanocrystals via interface nucleation is modified as follows

$$-\frac{dN}{dt} = \frac{f_0^{'}}{D_0^{6.7}} \exp\left(-\frac{E_a(\infty) + c/D_0}{RT}\right) \cdot N^2 \qquad (6)$$

where f'_0 is the pre-exponential factor that is now independent of the initial particle size.

It is well known that the anatase to rutile transformation is very strongly size dependent [12, 23]. However, the explanation for this phenomenon has remained unclear. Our results indicates that for transformations proceeding solely by interface nucleation, f_0

may increase by ~$10^{3.7}$ times in 10 nm compared to in 100 nm anatase particles and by ~$10^{7.4}$ for 1 μm sized particles (i.e., the size at which the transformation via interface nucleation would not be expected at < 600 °C). Because the concentration of interface nucleation sites ($N_1 \propto 1/D_0^3$) can control the transformation kinetics in nanocrystals, synthesis conditions may be modified to manipulate the aggregation state (e.g. in nonaqueous solutions, synthesized nanocrystalline anatase is only slightly aggregated [24]), and thus the phase content and particle size, and materials properties.

Conclusions

In this work, we explored the quantitative relationship between the kinetic rate constant and particle size for phase transformation in nanocrystalline anatase via interface nucleation at particle-particle contacts at temperatures below 600 ^{o}C. Arrhenius analyses of the rate constants derived by kinetic modeling of the experimental data revealed that the activation energy increases slightly with decreasing particles size of anatase, but the pre-exponential factor increases dramatically as the particle size decreases. The high concentration of particle-particle contacts per unit volume in small anatase accounts primarily for the large pre-exponential factor. A kinetic equation with the rate constant expressed explicitly as functions of both temperature and particle size was given for phase transformation in nanoparticles controlled by interface nucleation. The findings of this study may provide useful instructions to the fabrication of nanoparticulate TiO_2 products with desired phase contents and structure.

Acknowledgements. We thank Drs. B. Gilbert, Q. Jin, B. Chen, and F. Huang for discussions. This work was supported by the US National Science Foundation (grant # EAR-0123967) and the US Department of Energy (grant # DE-FG03-01ER15218).

Supporting Information Available: Kinetic data and kinetic plots for phase transformation from nanocrystalline anatase to rutile at temperatures 480, 500, 540, 560 and 580 ^{o}C; Adsorption / desorption isotherms, specific surface areas and cumulative pore areas of anatase samples. This material is available free of charge via the Internet at http://pubs.acs.org.

References

1. Gnaser, H.; Huber, B.; Ziegler, C. *Encycl. Nanosci. Nanotech.* **2004**, *6*, 505.

2. Gao, L.; Zhang, Q. *Scr. Mater.* **2001**, *44*, 1195.

3. Ray, C. S.; Huang, W.; Day, D. E. *J. Am. Ceram. Soc.* **1991,** *74*, 60.

4. Ozturk, A. *Phys. Chem. Glasses* **2000**, *41*, 71.

5. Jacobs, K; Zaziski, D.; Scher, E. C.; Herhold, A. B.; Alivisatos, A. P. *Science* **2001,** *293*, 1803.

6. Tolbert, S. H.; Alivisatos, A. P. *Annual Rev. of Phys. Chem.* **1995,** *46*, 595.

7. Tolbert, S. H.; Alivisatos, A. P. *J. Chem. Phys.* **1995**, *102*, 4642.

8. Gilbert , B.; Zhang , H.; Huang, F.; Finnegan, M. P.; Waychunas, G. A.; Banfield, J. F. *Geochem. Trans.* **2003,** *4*, 20.

9. Zhang, H.; Banfield, J. F. *Am. Miner.* **1999,** *84*, 528.

10. Zhang, H.; Banfield, J. F. *J. Mater. Res.* **2000**, *15*, 437.

11. Zhang, H.; Finnegan, M.; Banfield, J. F. *Nano Lett.* **2001**, *1*, 81.

12. Gribb, A. A.; Banfield, J. F. *Am. Miner.* **1997**, *82,* 717.

13. Barrett, E. P.; Joyner, L. S.; Halenda, P. P. *J. Am. Chem. Soc.* **1951,** *73*, 373.

14. Shuttleworth, R. *Proc. Phys. Soc. London* **1950,** *A63*, 444.

15. Cammarata, R. C.; Sieradzki, K. *Annu. Rev. Mater. Sci.* **1994**, *24*, 215.

16. Cheng, B.; Kong J.; Luo, J.; Dong, Y. *Mater. Sci. Progress* (Chinese) **1993**, *7*, 240.

17. Chen, L. X.; Rajh, T.; Jager, W.; Nedeljkovic, J.; Thurnauer, M. C. *J. Synchrotron Rad.* **1999**, *6*, 445.

18. Talapin, D. V.; Rogach, A. L.; Hasse, M.; Weller, H. *J. Phys. Chem. B* **2001,** *105*, 12278.

19. Atkins, P. *Physical Chemistry (5th edition);* W. H. Freeman and Company: New York, **1994**.

20. Gilbert, B.; Huang, F.; Zhang, H.; Waychunas, G. A.; Banfield, J. F. *Science* **2004,** *305*, 651.

21. Penn, R. L.; Banfield, J. F. *Am. Miner.* **1999**, *84*, 871.

22. Higgins, K. J.; Jung, H.; Kittelson, D. B.; Roberts, J. T.; Zachariah, M. R. *J. Phys. Chem. A* **2002**, *106*, 96.

23. Banfield, J. F.; Bischoff, B. L.; Anderson, M. A. *Chem. Geo.* **1993,** *110*, 211.

24. Niederberger, M.; Bartl, M. H. ; Stucky, G. D. *Chem. Mater.* **2002,** *14*, 4364.

Figure Captions

Figure 1. Experimental data and kinetic plots for phase transformation in nanocrystalline anatase. a, The weight percentages of rutile, b, the average particle sizes of anatase, and c, the kinetic plots (eq 1b) of experimental data at 520 ^{o}C. Lines in (c) are from linear least square regressions (the last two data points at $\ln(t) > 3.5$ were not included in each regression because at a longer reaction time nanoparticle coarsening may become significant and induce deviation of the plot from the linear relationship as given by eq 1b; see ref.9). Legends for initial particle sizes of anatase are depicted in (a) and also applicable to (b) and (c).

Figure 2. Variations of kinetic constant and parameter with temperature and initial particle size of anatase. a, The Arrhenius plot of the rate constant as a function of the initial particle size (ref. Figure 1a for legends of the sizes). b, The activation energy vs. the reciprocal initial particle size. c, log–log plot of the apparent pre-exponential factor vs. the initial particle size. Solid lines are from linear least square regressions. Errors bars indicate the standard deviations.

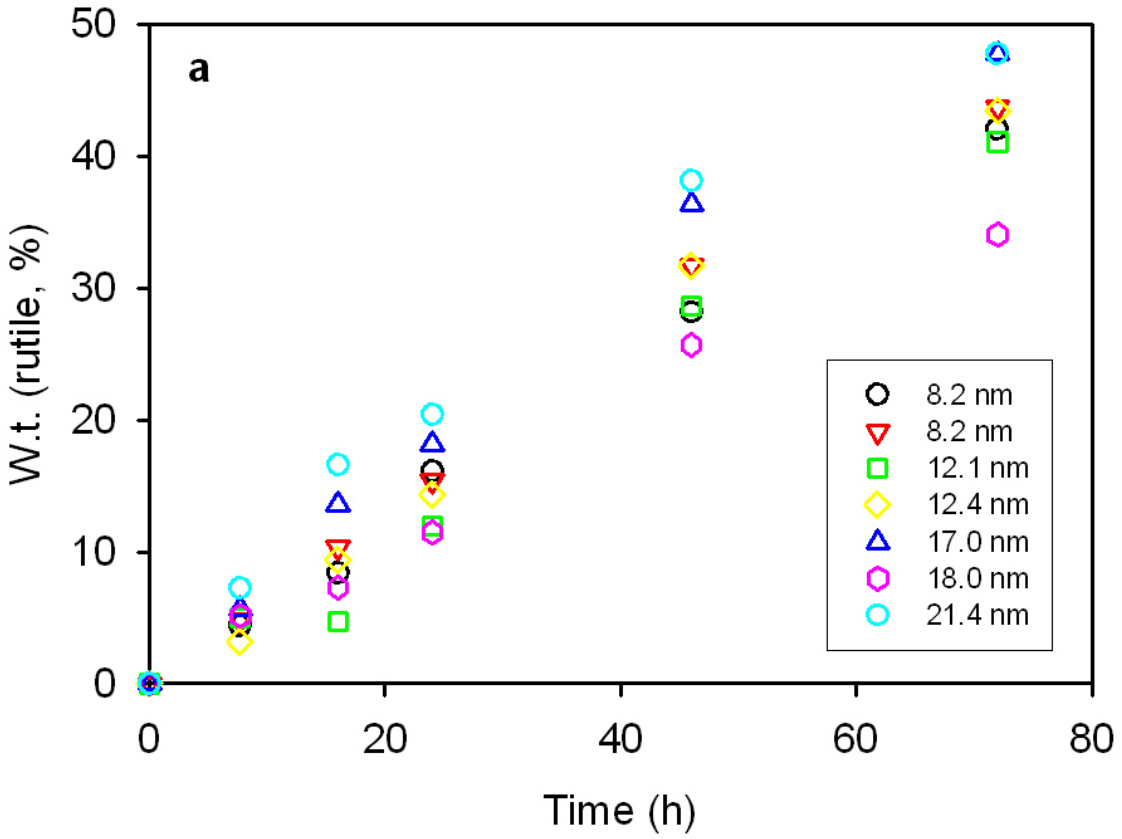

Figure 1a (Zhang and Banfield)

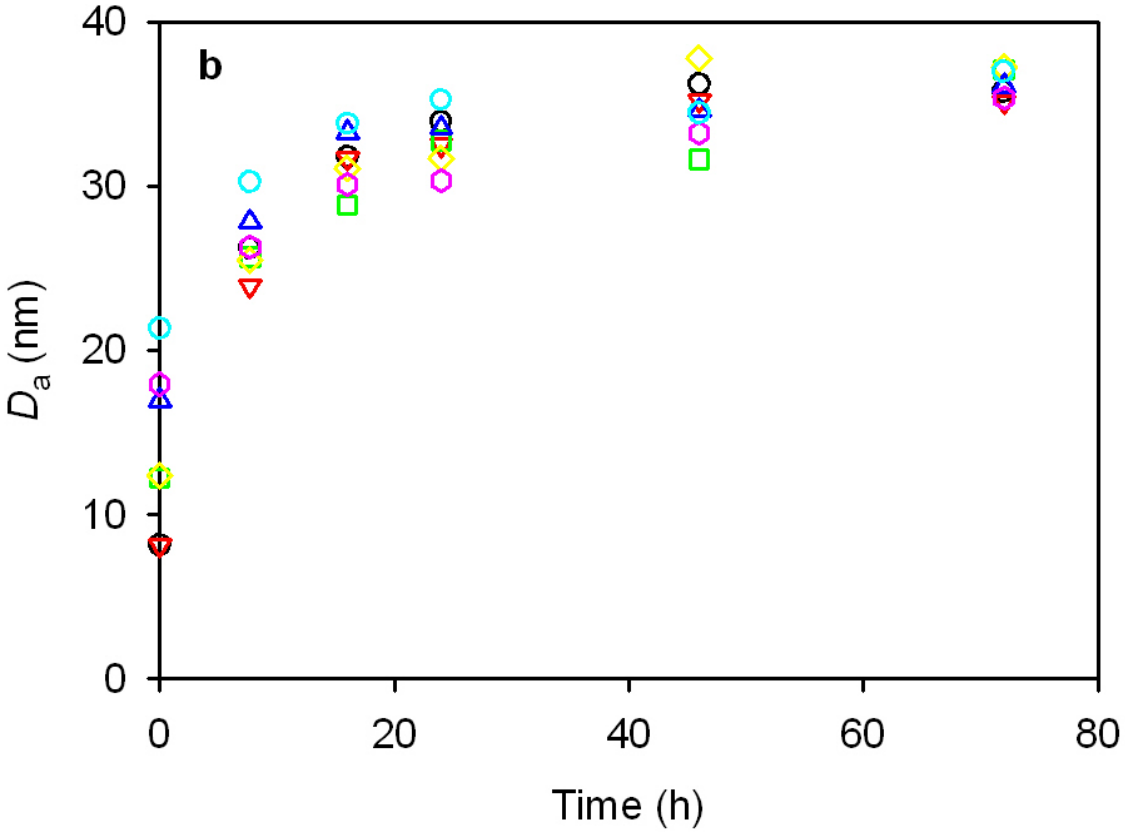

Figure 1b (Zhang and Banfield)

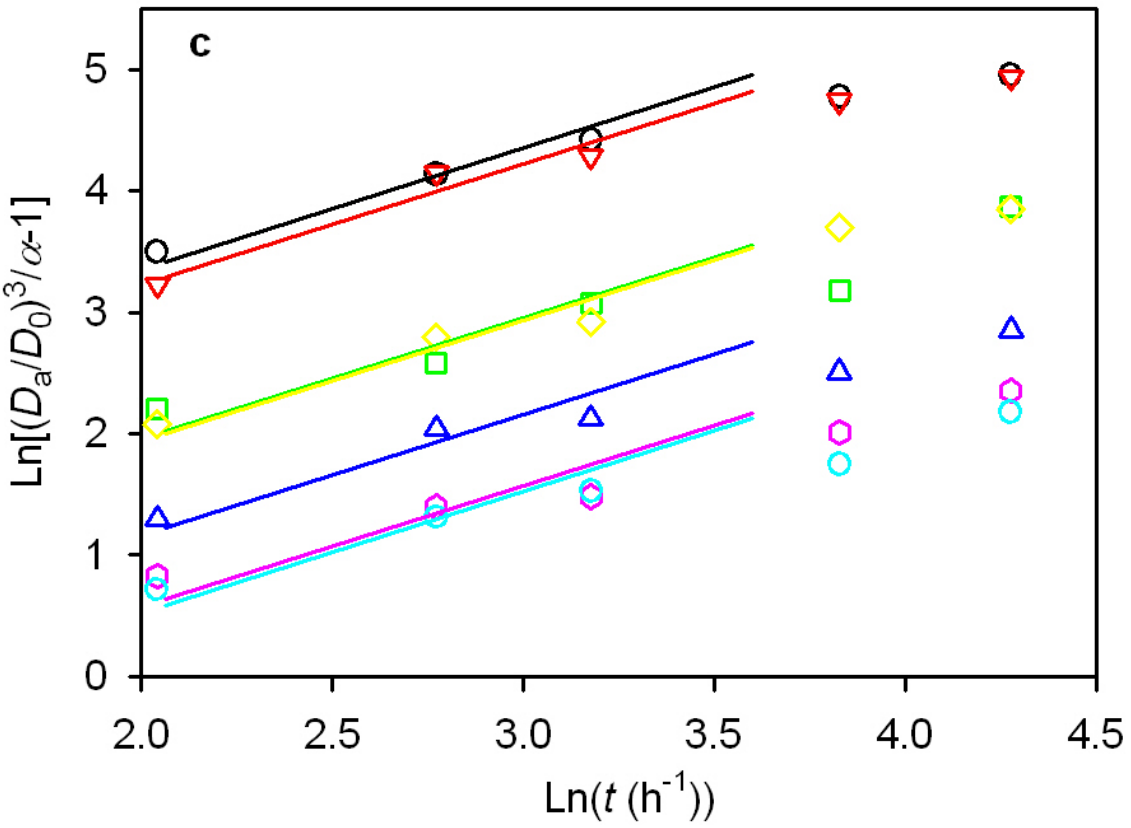

Figure 1c (Zhang and Banfield)

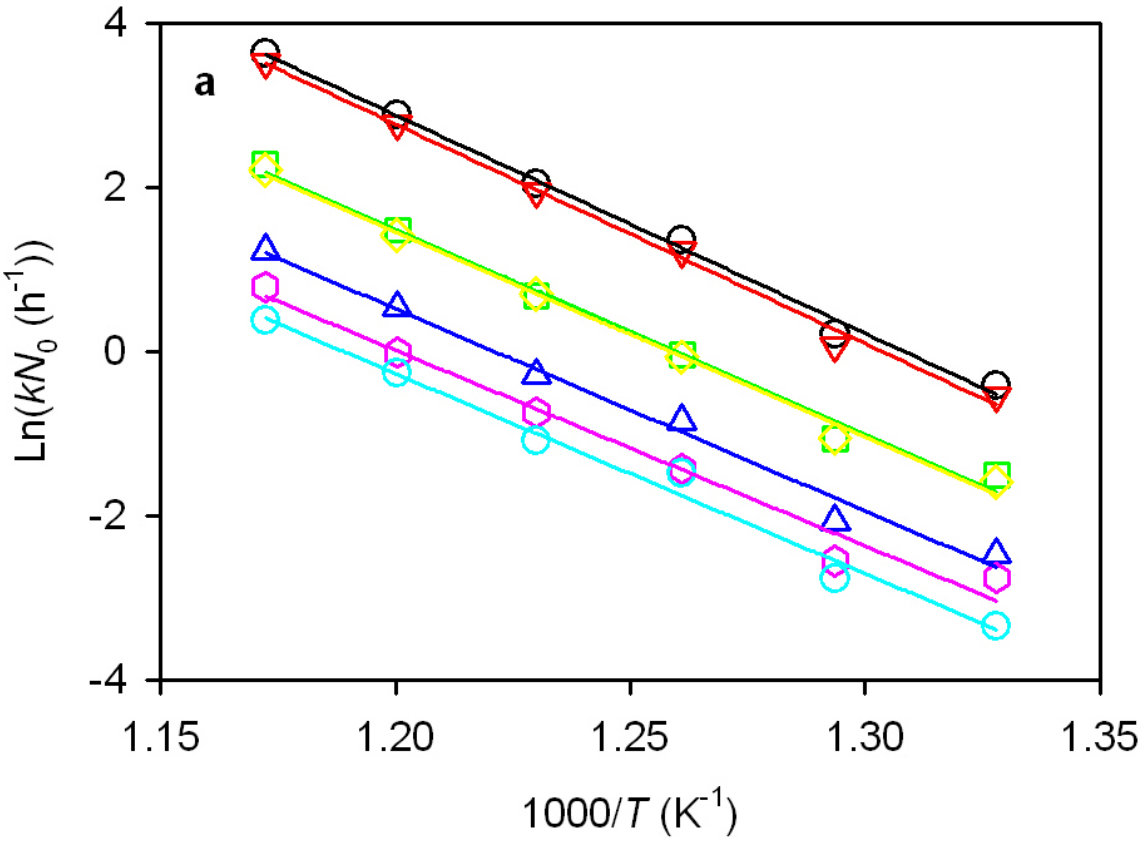

Figure 2a (Zhang and Banfield)

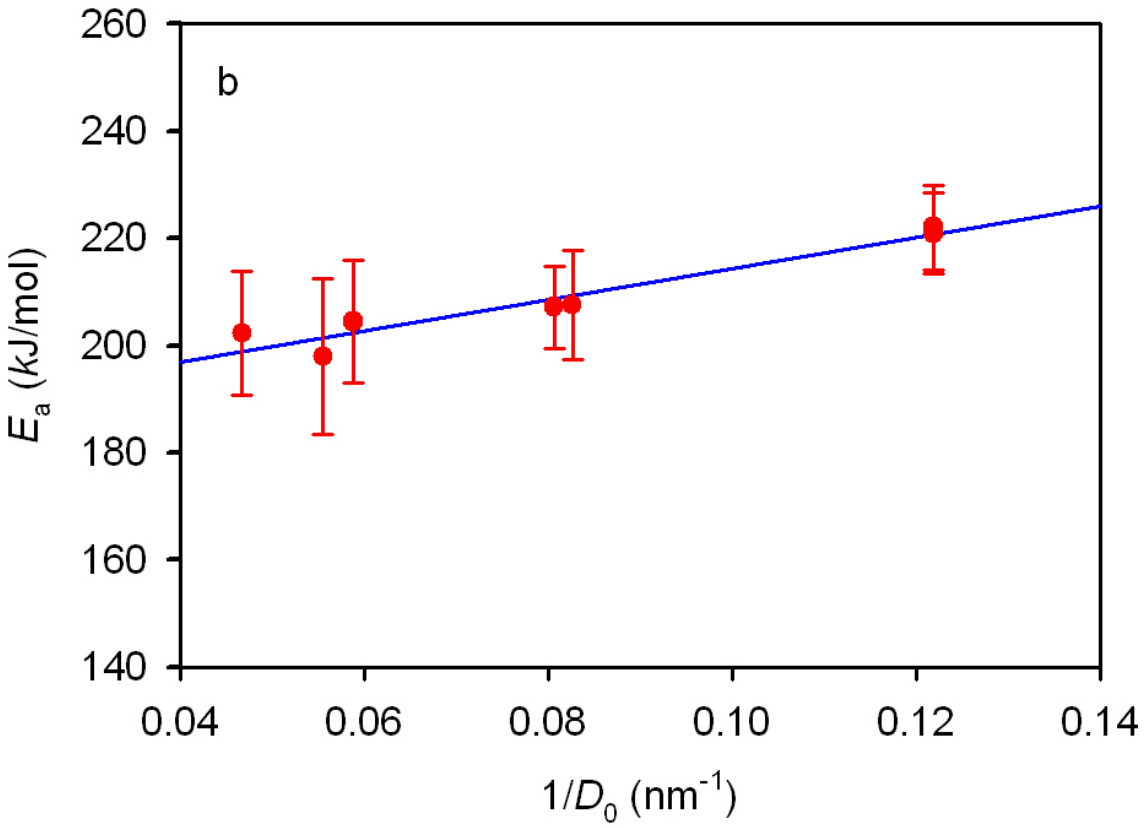

Figure 2b (Zhang and Banfield)

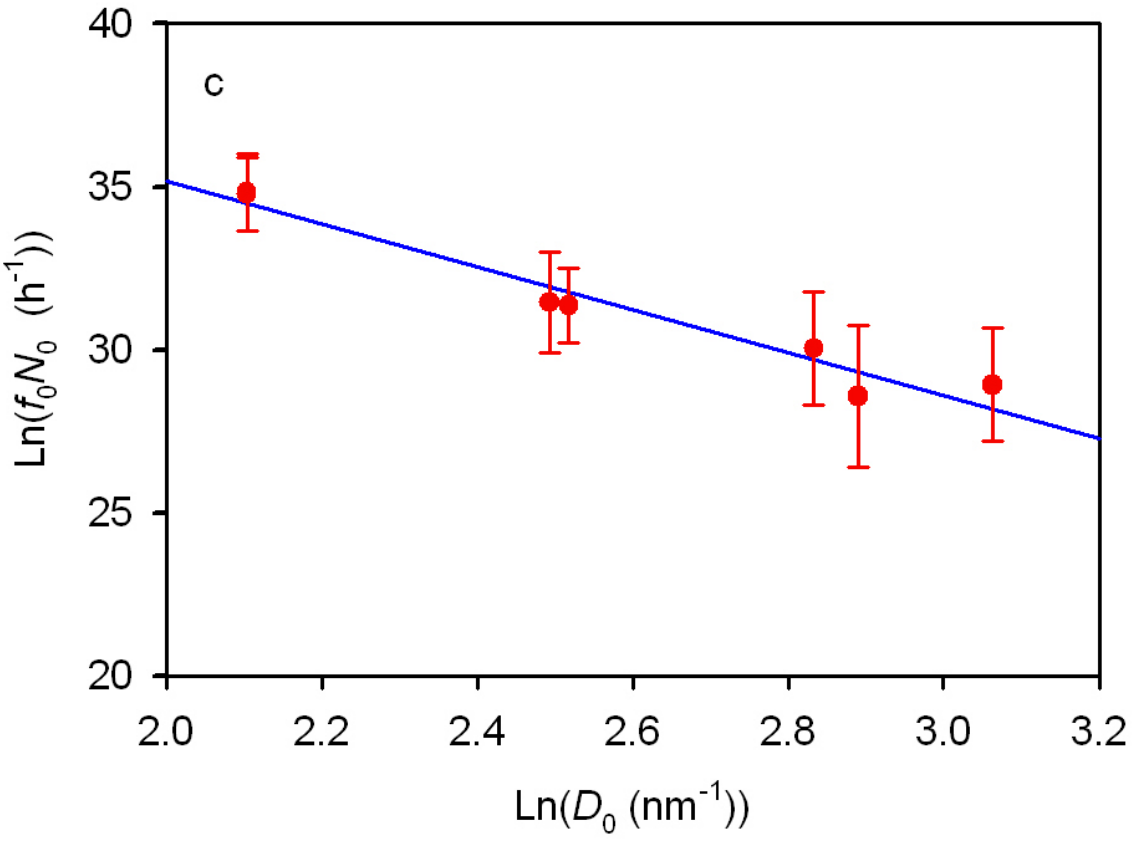

Figure 2c (Zhang and Banfield)